

Self-Assembled Monolayer-Based Hole-Transporting Materials

Subjects: Chemistry, Organic

Contributor: Doyeong Yeo, Juyeon Shin, Dabit Kim, Jae Yun Jaung, In Hwan Jung

Ever since self-assembled monolayers (SAMs) were adopted as hole-transporting layers (HTL) for perovskite solar cells (PSCs), numerous SAMs for HTL have been synthesized and reported. SAMs offer several unique advantages including relatively simple synthesis, straightforward molecular engineering, effective surface modification using small amounts of molecules, and suitability for large-area device fabrication.

Keywords: self-assembled monolayers ; hole-transporting materials ; perovskite solar cells

1. Introduction

Perovskite crystals are one of the hottest materials for solution-processible electronic devices such as solar cells, photodetectors, transistors, and light-emitting diodes due to their high performance, which is comparable to that of existing silicon-based devices [1][2][3][4][5][6][7][8][9][10][11][12][13][14]. Among the various applications, perovskite solar cells (PSCs) have achieved remarkable progress, and the power conversion efficiency (PCE) of PSCs has dramatically increased over the past decade, now reaching a PCE value of 25.2%, which is comparable to that of commercialized silicon solar cells [15][16][17][18][19][20][21][22][23][24]. After the first report on PSCs in 2009 [25], there have been many attempts to improve the efficiency and long-term stability of PSCs, such as interface engineering, perovskite composition optimization and encapsulation techniques, and so on [26][27][28][29][30]. Among those attempts, modifying interfacial layers such as the hole-transporting layer (HTL) and the electron-transporting layer (ETL) has also been widely studied. These modifications enhance the charge transfer at the interface of the electrodes and directly affect the growth of perovskite crystals on the active layer [31][32][33][34].

Both inorganic and organic materials have been developed as hole-transporting materials (HTMs) for inverted PSCs. In the case of inorganic HTMs, copper(I) iodide (CuI), copper(I) thiocyanate (CuSCN), copper oxides (Cu₂O and CuO), and nickel oxide (NiO) are currently being developed, with the great advantages of low production costs, high hole mobility, and chemical stability [35]. However, there are some limitations related to adjusting energy levels and solution processability [36]. In the case of organic HTMs, they require multiple synthetic steps from commercially available organic chemicals, but it is easy to diversify the molecular structures of materials, which allows for the fine-tuning of energy levels. In addition, they have the unique advantages of being light-weight, having a less-adverse environmental impact, and solution processability [37]. There are roughly two types of organic HTMs: (1) one comprises conventional polymer or small-molecule HTMs forming their own energy levels, and (2) the other includes small-molecule HTMs making self-assembled monolayers (SAM) capable of modifying the energy levels of electrodes. The well-known polymer-type HTMs are PTAA and PEDOT:PSS, which all possess excellent electrical conductivity with proper HOMO energy levels, facilitating hole transport from the perovskite layer to the electrode [38][39][40][41]. However, those HTMs should be deposited to a thickness of several tens of nanometers for film uniformity, and their HOMO levels and hole mobilities must be well controlled for the efficient transport of charge [42][43][44]. On the contrary, SAM-based HTMs are extremely thinly coated on the transparent conductive oxide (TCO) electrodes, forming a permanent dipole moment at the interfaces, which effectively modulates the work function (WF) of the electrode [45][46][47][48].

2. SAM-Based HTMs

2.1. Structure and Characteristics of SAM-Based HTMs

The structure of the HTMs forming SAMs is categorized into three components, as shown in **Figure 1**. The first part is a head group in direct contact with the perovskite layer. Head groups are typically composed of hydrophobic conjugated molecules, such as triphenyl amine, carbazole, and phenothiazine, which improve contact with the perovskite layer compared to bare TCO [49]. The second part is an anchoring group that binds to the TCO electrodes, such as indium tin

oxide (ITO) or fluorine-doped tin oxide (FTO). The interaction between the anchoring group and the TCO creates an induced electric field at the interfaces, which down-shift the WF (increase the effective WF, ϕ_{eff}) of the TCO for efficient hole transport [34][50]. There are various anchoring groups, such as PA, CA, CAA, $\text{B}(\text{OH})_2$, and $-\text{SO}_3\text{H}$.

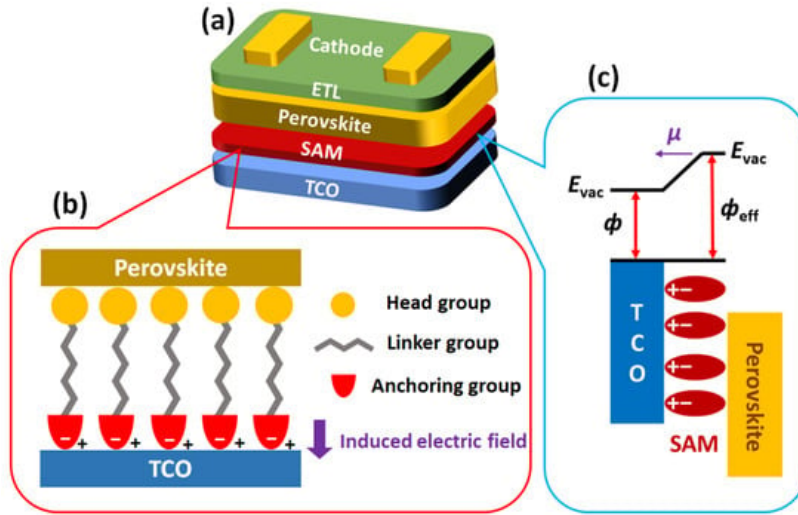


Figure 1. (a) The general device structure of inverted PSCs, (b) three components of HTMs forming SAM and their location in the PSCs, and (c) the modification of WF by SAM.

The synthesis of SAMs starts with the design of the core head group, which primarily employs electron-donating moieties. After that, the anchoring group is introduced into the head group with a proper space linker. The synthetic routes required to build SAM-based HTMs are mainly determined depending on the anchoring groups, and, thus, scholars categorized them by the anchoring groups, as follows. (1) PA anchoring group: First, the electron-donating core unit is brominated, and then it reacts with triethylphosphate to produce phosphonate. Then, a hydrolysis procedure is subsequently used to convert it to phosphonic acid. (2) CA anchoring group: CA anchoring groups can be incorporated into SAM-based HTMs in two different ways. The first way is introducing a benzoic acid group at the end of the HTMs. The head and linker are connected first, and then alkyl benzoate is reacted with by C-C coupling in the presence of a palladium catalyst. Subsequently, the resulting compound undergoes hydrolysis, followed by an acid treatment, to ultimately convert the ester group into a CA group. The second way consists of introducing an aliphatic CA to the HTMs. The aliphatic ester is alkylated to the electron-rich head group, usually including amine derivatives. The ester group is transformed into a CA group through a saponification reaction. (3) CAA anchoring group: Initially, an aromatic aldehyde is linked to the electron-rich head group via palladium-catalyzed C-C coupling. And then, a CAA group is easily introduced into the resulting compound through Knoevenagel condensation.

2.2. PA-Based SAMs

The PA group has been demonstrated to create strong and stable bindings on TCO surfaces, enabling efficient WF modifications [51][52]. This group contains two hydroxy groups and one phosphonic group, allowing for three different binding modes depending on the substrate surfaces and reaction conditions [36]. Among various anchoring groups, the PA group exhibited the highest bond energy, especially with TiO_2 surfaces [53]. These strong bonds contribute to an exceptional monolayer stability. Consequently, the PA group is considered to be one of the most powerful anchoring groups for SAMs, and numerous SAMs have been synthesized with this group in order to be used as HTMs for PSCs (**Figure 2**). The photovoltaic properties of PSCs are summarized in **Table 1**.

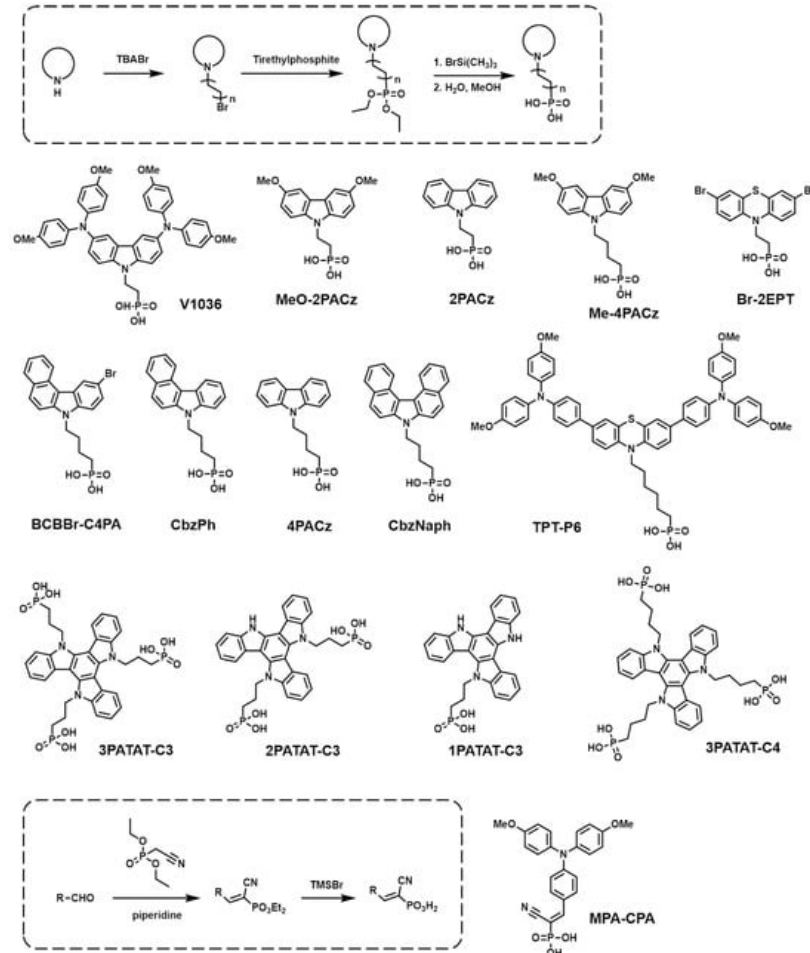


Figure 2. General synthetic routes and molecular structures of **PA** anchoring group-based SAMs.

Table 1. Photovoltaic properties of PSCs using **PA**-based SAMs.

HTM	Device Structure	V _{OC} [V]	J _{SC} [mA/cm ⁻²]	FF [%]	PCE [%]	Device Stability ^a	Refs.
V1036	ITO/V1036/C4/Cs _{0.05} (MA _{0.17} FA _{0.83}) _{0.95} Pb(I _{0.83} Br _{0.17}) ₃ /C ₆₀ /BCP/Cu	1.09	21.9	81.0	17.8	~94%, 180 d, RT ^{b,f}	[54]
MeO- 2PACz	ITO/MeO- 2PACz/Cs _{0.05} (MA _{0.17} FA _{0.83}) _{0.95} Pb(I _{0.83} Br _{0.17}) ₃ /C ₆₀ /BCP/Cu	1.144	22.2	79.3	19.2	>97%, 11 h, ~40 °C ^{c,f}	[55]
2PACz	ITO/2PACz/C4/Cs _{0.05} (MA _{0.17} FA _{0.83}) _{0.95} Pb(I _{0.83} Br _{0.17}) ₃ /C ₆₀ /BCP/Cu	1.188	21.9	80.2	20.9	~97%, 11 h, ~40 °C ^{c,f}	
Me- 4PACz	ITO/Me- 4PACz/Cs _{0.05} (FA _{0.77} MA _{0.23}) _{0.95} Pb(I _{0.77} Br _{0.23}) ₃ /C ₆₀ /SnO ₂ /Ag	1.15	20.3	84	20.0	95.5%, 300 h, RT ^{c,d,g}	[56]
Br-2EPT	ITO/Br-2EPT/Cs _{0.05} (FA _{0.92} MA _{0.08}) _{0.95} Pb(I _{0.92} Br _{0.08}) ₃ /C ₆₀ /BCP/Cu	1.09	25.11	82.0	22.44	107.4%, 100 h, RT ^{c,e,g}	[57]
BCBBr- C4PA	ITO/BCBBr-C4PA/FA _{0.8} Cs _{0.2} Pb(I _{0.6} Br _{0.4}) ₃ /C ₆₀ /ALD-SnO ₂ /Cu	1.286	17.54	82.61	18.63	>90%, 250 h ^{c,f}	[58]
CbzPh	ITO/CbzPh/Cs _{0.05} MA _{0.15} FA _{0.80} PbI ₃ /C ₆₀ /BCP/Ag	1.17	23.43	73.06	19.2	91%, 120 h ^{c,f}	
CbzNaph	ITO/CbzNaph/Cs _{0.05} MA _{0.15} FA _{0.80} PbI ₃ /C ₆₀ /BCP/Ag	1.17	24.69	83.39	24.1	97%, 120 h ^{c,f}	[59]
4PACz	ITO/4PACz/Cs _{0.05} MA _{0.15} FA _{0.80} PbI ₃ /C ₆₀ /BCP/Ag	1.07	23.20	58.43	14.5	88%, 120 h ^{c,f}	

HTM	Device Structure		V _{oc} [V]	J _{sc} [mA/cm ⁻²]	FF [%]	PCE [%]	Device Stability a	Refs.
TPT-P6	ITO/TPT-P6/Cs _{0.05} MA _{0.12} FA _{0.83} Pb(I _{0.85} Br _{0.15}) ₃ /C ₆₀ /BCP/Ag		1.125	23.20	80.38	20.77	>90%, 200 h c,d,g	[60]
MPA-CPA	ITO/MPA-CPA/Cs _{0.05} (FA _{0.95} MA _{0.05}) _{0.95} Pb(I _{0.95} Br _{0.05}) ₃ /C ₆₀ /BCP/Ag		1.20	24.8	84.5	25.16	>90%, 2000 h, ~45 °C c,d,g	[61]
3PATAT-C3	ITO/3PATAT-C3/Cs _{0.05} FA _{0.80} MA _{0.15} PbI _{2.75} Br _{0.25} /EDAI2/C ₆₀ /BCP/Ag		1.13	24.5	83	23.0	~100%, 2000 h, RT b,f	
2PATAT-C3	ITO/2PATAT-C3/Cs _{0.05} FA _{0.80} MA _{0.15} PbI _{2.75} Br _{0.25} /EDAI2/C ₆₀ /BCP/Ag		1.14	23.3	83	22.2	-	[62]
1PATAT-C3	ITO/1PATAT-C3/Cs _{0.05} FA _{0.80} MA _{0.15} PbI _{2.75} Br _{0.25} /EDAI2/C ₆₀ /BCP/Ag		1.06	24.0	82	21.1	-	

References

1. Zhang, H.; Pfeiffer, C.; Zeng, X.; Madaeni, S.; Mørk, G.; Grancini, G.; Goriely, A.; Dittmar, T. Tailoring passivators for highly efficient and stable perovskite solar cells. *Nat. Rev. Chem.* 2023, 7, 632–652.
2. Park, S.M.; Wei, M.; Xu, J.; Atapattu, H.R.; Eickemeyer, F.T.; Darabi, K.; Grater, L.; Yang, Y.; Liu, C.; Teale, S.; et al. Maintained performance of its initial PCE after a specific time, ^b dark condition, ^c simulated 1 sun AM 1.5G illumination; ^d relative humidity 30–40%; ^e relative humidity 15–25%; ^f inert gas; ^g ambient air. *Science* 2023, 381, 209–215.

2.3 CA-Based SAMs

The CA group is well-known for its strong binding affinity to metal oxides like ZnO and ITO, and the CA-based surface modifiers have demonstrated excellent performance in organic solar cells ^[63]. Moreover, due to the electron-withdrawing property of the CA group, it creates a strong dipole moment when combined with electron-rich moieties ^[65]. This characteristic ^a relatively easily ^b modify the perovskite electrode, ^c significantly ^d improve the hole transporting properties ^e transistors as ^f electron-transporting layer in PSCs ^[66]. Recently, various research results have also been reported on their use as HTMs in PSCs (Figure 3). The photovoltaic properties of PSCs are summarized in Table 2.

Nanomaterials 2023, 13, 2024.

7. Petrović, M.; Chellappan, V.; Ramakrishna, S. Perovskites: Solar cells & engineering applications—Materials and device developments. *Sol. Energy* 2015, 122, 678–699.

8. Wu, T.; Qin, Z.; Wang, Y.; Wu, Y.; Chen, W.; Zhang, S.; Cai, M.; Dai, S.; Zhang, J.; Liu, J. The main progress of perovskite solar cells in 2020–2021. *Nano-Micro Lett.* 2021, 13, 152.

9. Maafa, I.M. All-inorganic perovskite solar cells: Recent advancements and challenges. *Nanomaterials* 2022, 12, 1651.

10. Jeong, W.; Ha, S.R.; Jang, J.W.; Jeong, M.-K.; Hussain, M.D.W.; Ahn, H.; Choi, H.; Jung, I.H. Simple-Structured Low-Cost Dopant-Free Hole-Transporting Polymers for High-Stability CsPbI₂Br Perovskite Solar Cells. *ACS Appl. Mater. Interfaces* 2022, 14, 13400–13409.

11. Paulus, F.; Tyznik, C.; Jurchescu, O.-D.; Vaynzof, Y. Switched-On: Progress, Challenges, and Opportunities in Metal Halide Perovskite Transistors. *Adv. Funct. Mater.* 2021, 31, 2101029.

12. Zhang, Y.; Zhao, Z.; Liu, Z.; Tang, A. The Scale Effects of Organometal Halide Perovskites. *Nanomaterials* 2023, 13, 2935.

13. Li, G.; Wang, Y.; Huang, L.; Sun, W. Research Progress of High-Sensitivity Perovskite Photodetectors: A Review of Photodetectors: Noise, Structure, and Materials. *ACS Appl. Electron. Mater.* 2022, 4, 1485–1505.

14. Lu, X.; Li, J.; Zhang, Y.; Han, Z.; He, Z.; Zou, Y.; Xu, X. Recent progress on perovskite photodetectors for narrowband detection. *Adv. Photonics Res.* 2022, 3, 2100335.

15. Yang, T.; Gao, L.; Lu, J.; Ma, C.; Du, Y.; Wang, P.; Ding, Z.; Wang, S.; Xu, P.; Liu, D.; et al. One-stone-for-two-birds strategy to attain beyond 25% perovskite solar cells. *Nat. Commun.* 2023, 14, 839.

16. Correa-Baena, J.-P.; Saliba, M.; Buonassisi, T.; Grätzel, M.; Abate, A.; Tress, W.; Hagfeldt, A. Promises and challenges of perovskite solar cells. *Science* 2017, 358, 739–744.

17. Kim, J.Y.; Lee, J.-W.; Jung, H.S.; Shin, H.; Park, N.-G. High-Efficiency Perovskite Solar Cells. *Chem. Rev.* 2020, 120, 7867–7918.

18. Sabbah, H.; Figure 8; General Synthesis and Characterization of 26% EDAI2 and Post-treated SAMs for Perovskite Solar Cells Based on $\text{GA}_0.2\text{FA}_0.78\text{SnI}_3$ -1%EDAI2 Films. *Nanomaterials* 2022, 12, 3885.

19. Li, H.; Zhang, W. Perovskite Tandem Solar Cells: From Fundamentals to Commercial Deployment. *Chem. Rev.* 2020, 120, 9835–9950.

HTM	Device Structure	Voc	Jsc	FF	PCE	Device Stability	Refs.
20. Wu, X.; Li, B.; Zhu, Z.; Chueh, C.-C.; Jen, A.K.Y. Designs from Single-junctions ^a to Heterojunctions ^b to Stabilizations for high-performance perovskite solar cells. <i>Chem. Soc. Rev.</i> 2021, 50, 13090–13128.	ITO/MC- MC-43	1.07	20.3	80.0	17.3	90%, 20 d ^b	[67]
21. Asmontas, S.; Majumder, M. Recent Progress in Tandem Solar Cells. <i>Nanomaterials</i> 2023, 13, 1886.	ITO/EA-44/MAPI ₃ /PCBM/Ca/Ag	1.024	17.95	68.15	12.03	-	[68]
22. EAT-1P.; Sangale, S.; ISO/EA-44/MAPI ₃ /PCBM/Ca/Ag. Photovoltaic Approaches to 37.8% Transparency Perovskite Solar Cells. <i>Nanomaterials</i> 2023, 13, 1084.	ITO/EA-46/MAPI ₃ /PCBM/Ca/Ag	1.006	15.70	62.18	10.24	-	
23. Lye, Y.-E.; Chan, K.-Y.; Ng, Z.-N. A Review on the Progress, Challenges, and Performances of Tin-Based Perovskite Solar Cells. <i>Nanomaterials</i> 2023, 13, 585.	ITO/EA-49/MAPI ₃ /PCBM/Ca/Ag	1.023	15.70	56.56	8.71	-	[69]
24. Isikgor, F.H.; Zhumagali, S.T.; Merino, L.V.; De Bastiani, M.; McCulloch, I.; De Wolf, S. Molecular engineering of contact interfaces for high-performance perovskite solar cells. <i>Nat. Rev. Mater.</i> 2023, 8, 89–108.	ITO/EA-50/MAPI ₃ /PCBM/Ca/Ag	1.035	16.91	56.30	9.09	-	
25. Kojima, A.; Teshima, K.; Shirai, Y.; Miyasaka, T. Organometal halide perovskites as visible-light sensitizers for photovoltaic cells. <i>J. Am. Chem. Soc.</i> 2009, 131, 6050–6051.	ITO-co-assembled TPA-PTC	1.04	21.8	77.4	17.19	89%, 220 h, c,e,g	[68]
26. Chi, W.; Banerjee, S. Stability Improvement of Perovskite Solar Cells by Compositional and Interface Engineering. <i>Adv. Mater.</i> 2021, 33, 1500070.	ITO/EADRO3	1.156	22.9	80.0	21.2	91%, 200 h, RT c,f	[69]
27. Azmi, R.; Lee, T.O.; EADRO4. <i>Cs_{0.16}SnI₃(MAI)_{0.16}Br_{0.16}</i> . Improvement in efficiency and stability of low-temperature-processed perovskite solar cells by interfacial control. <i>Adv. Energy Mater.</i> 2018, 8, 1702934.	ITO/LiF/C ₆₀ /BCP/NaF/Cu	1.164	22.6	80.0	21.0	91%, 250 h, RT c,f	
28. Azmi, R. Highly-transparent Perovskite Tandem Films Obtained by a Wet Chemical Processing Method. <i>Non-Met. Mater. Sci.</i> 2019, 1, 22–27.	ITO/RC-24/CsFAMA/C ₆₀ /BCP/Cu	1.12	22.3	79	19.8	97%, 120 s	[70]
29. Alzoubi, T.; Mourched, B.; Al Gharram, M.; Makhadmeh, G.; Abu Noqta, O. Improving Photovoltaic Performance of Hybrid Organic-Inorganic MAGel3 Perovskite Solar Cells via Numerical Optimization of Carrier Transport Materials (HTLs/ETLs). <i>Nanostruct. Mater.</i> 2018, 29, 115–120.	ITO/RC-34/CsFAMA/C ₆₀ /BCP/Cu	1.11	22.5	79	19.7	95%, 120 s	
30. Liu, H.; Xiang, L.; Gao, P.; Wang, D.; Yang, J.; Chen, X.; Li, S.; Shi, Y.; Gao, F.; Zhang, Y. Improvement strategies for stability and efficiency of perovskite solar cells. <i>Nanomaterials</i> 2022, 12, 3895.	ITO/AC-16/CsFAMA/C ₆₀ /BCP/Ag	1.042	23.14	74.16	18.87	85%, 30 d, RT b,d,g	[60]
31. Jeong, M.-K.; Kang, J.; Park, D.; Yim, S.; Jung, I.H. A conjugated polyelectrolyte interfacial modifier for high performance near-IR perovskite solar cells. <i>J. Mater. Chem. B</i> 2020, 8, 2542–2550.	ITO/AC-17/CsFAMA/PCBM/BCP	-	-	-	-	90%, 30 d, RT b,d,g	[71]
32. Azmi, R.; Lee, U.-H.; Wibowo, F.T.A.; Eom, S.H.; Yoon, S.C.; Jang, S.-Y.; Jung, I.H. Performance improvement in low-temperature-processed perovskite solar cells by molecular engineering of porphyrin-based hole-transport materials. <i>ACS Appl. Mater. Interfaces</i> 2018, 10, 35404–35410.	ITO/AC-18/CsFAMA/PCBM/BCP/PhBiphenyl	1.130	24.42	84.95	23.19	91%, 30 d, RT b,d,g	
33. Lee, U.H.; Azmi, R.; Sirigama, S.; Hwang, S.; Eom, S.H.; Kim, T.W.; Poon, S.C.; Jang, S.Y.; Jung, I.H. Diphenyl-2-Spiro-Acid and 1,4-Diphenyl-2-pyridylamine-Substituted Porphyrins as Hole-Transporting Materials for Perovskite Solar Cells. <i>ChemSusChem</i> 2017, 10, 3780–3787.	ITO/Spiro-Acid/C ₆₀ (FA _{0.05} MA _{0.05}) _{0.90} PhBiphenyl	0.990	22.20	82.6	18.15	=100%, 100 d	[72]
34. Azmi, R.; Sirigama, S.; Akbar, Z.A.; Lee, C.-L.; Yoon, S.C.; Jung, I.H.; Jang, S.-Y. High-performance dopant-free conjugated small molecule-based hole-transport materials for perovskite solar cells. <i>Nano Energy</i> 2018, 44, 191–198.	a) maintained performance of its initial PCE after a specific time; b) dark condition; c) simulated 1 sun AM 1.5G illumination; d) relative humidity 20–30%; e) relative humidity 30–40%; f) inert gas; g) ambient air.						

35. Although CAA includes the CA part, it was discussed separately because the synthesis of CA-based SAMs is completely different from that of CA-based SAMs. The CAA group efficiently passivates the perovskite film because the Lewis base characteristics of CAA can trigger a coordination interaction with Pb^{2+} ion defects [73]. Furthermore, the CAA group has a stronger electron-withdrawing property than the CA group because it contains two electron-accepting moieties, -COOH and -CN. Thus, the combination with CAA and electron-donating head groups like carbazole and aryl amine forms a strong D-A structure, which is effective in enhancing hole extraction and reducing charge recombination in PSCs, making it suitable for PFM design [74]. The photovoltaic properties of PSCs are summarized in **Table 3**.

HTMP.; Other Structure	Device Structure	Voc	Jsc	FF	PCE	Device Stability	Refs.
40. HTMP.; Other Structure	M.I.; Xu, C.; Wang, X.; Tang, X. Electrical property modified hole transport layer (PEDOT:PMMA).	1.13	22.25	84.8	21.24	98%, 14 d,	
41. HTMP.; Other Structure	ITO/MPA-BT- MPA-C ₆₀ (FA _{0.17} MA _{0.34}) _{0.55} (3,11)-0.95/BCP/Ag	1.13	22.25	84.8	21.24	98%, 14 d,	[74]
42. HTMP.; Other Structure	Colella, S. Optimizing the interface between hole transporting material and nanocomposite for highly efficient perovskite solar cells. <i>Nanomaterials</i> 2019, 9, 1627.						

36. Yao, Y.; Cheng, C.; Zhang, C.; Hu, H.; Wang, K.; De Wolf, S. Organic hole-transport layers for efficient, stable, and durable perovskite solar cells. *Small Methods* 2018, 2, 1700280.

37. Anrango-Camacho, C.; Pavon-Ipiales, K.; Frontana-Uribe, B.A.; Palma-Cando, A. Recent advances in hole-transporting and -CN. Thus, the combination with CAA and electron-donating head groups like carbazole and aryl amine forms a layers for organic solar cells. *Nanomaterials* 2022, 12, 443.

38. Yin, X.; Song, Z.; Li, Z.; Tang, W. Toward ideal hole-transport materials: A review on recent progress in dopant-free hole transport materials for fabricating efficient and stable perovskite solar cells. *Energy Environ. Sci.* 2020, 13, 4057–4086.

39. Wang, Z.; Fan, P.; Zhang, D.; Yang, G.; Yu, J. Enhanced efficiency and stability of p-i-n perovskite solar cells using PMMA doped PTAA as hole transport layers. *Synth. Met.* 2020, 265, 116428.

40. HTMP.; Other Structure

41. HTMP.; Other Structure

		V_{oc} [V]	J_{sc} [mA/cm ²]	FF [%]	PCE [%]	Device Stability ^a	Refs.
42. Wang, S.; Guo, H.; Wu, Y. Advantages and challenges of self-assembled monolayer as a hole-selective contact for HTM Device Structure perovskite solar cells. <i>Mater. Futures</i> 2023, 2, 012105.							
43. Jiang, X.; Yu, Z.; Zhang, Y.; Lai, J.; Li, J.; Gurzadyan, G.G.; Yang, X.; Sun, L. High-Performance Regular Perovskite BTCA Cells Employing Low-Cost PCPDTB (Methylenedioxythiophene) as a Hole-Transporting Material. <i>Sci. Rep.</i> 2017, 7, 42564.	ITO/MPA-BT- BTCA	1.10	22.73	82.3	20.70	67%, 120 h, RT ^{b,g}	[74]
44. Zhang, F.; Yao, Z.; Guo, Y.; Li, Y.; Bergström, J.; Brett, C.J.; Cai, B.; Hajian, A.; Guo, Y.; Yang, X.; et al. Polymeric, Cost-Effective, Dopant-Free Hole Transport Materials for Efficient and Stable Perovskite Solar Cells. <i>J. Am. Chem. Soc.</i> 2019, 141(4), 19700–19707.	ITO/2FMPA-BT- 2FMPA	1.14	22.81	83.1	21.68	>74%, 120 h, RT ^{b,g}	[75]
45. Battelger, A.; Lee, S.G.; Park, S.G. Formation of Single-Chain Anionic Bolaamphiphiles on Indium Tin Oxide Surfaces through SAMs as (FA _{0.92} MA _{0.08}) _{0.95} PCPBM/C ₆₀ /Ag Performance. <i>ChemElectroChem</i> 2023, 10, e202300040.	TIO/CA- Cz-CA	-1.06	-23.2	-83.0	-20.0	-	
46. Ghiasiabi, K.; Zheng, X.; Turan, M.; Alipour, A.Y.; Lintangpradipto, M.N.; Yin, J.; Gutiérrez-Arzaluz, L.; Kotsovos, K.; Javal, A.; Gerigge, T.; et al. Hole-Transporting Self-Assembled Monolayer Enables Efficient Single-Crystal Perovskite Solar Cells with Enhanced Stability. <i>ACS Energy Lett.</i> 2023, 8, 950–956.	ITO/TPA- TPA-CA	-1.11	-23.0	-83.0	-20.2	-	
47. Wang, Z.; Lin, H.; Zhang, X.; Li, J.; Chen, X.; Wang, S.; Gong, W.; Yan, H.; Zhao, Q.; Lv, W. Revealing molecular transformation-induced stress at interlayered interfaces of organic optoelectronic devices by sum frequency generation Spectroscopy. <i>Synthetic Commun.</i> 2018, 48(19), 1855–1859.	ITO/Ph- Ph-CA	-1.06	-22.4	-81.0	-17.5	-	[76]
48. Mani, R.; Hattori, Y.; Matsunaga, S.; Maeda, G.; Pb(MnO ₂) ₃ /PCBM/C ₆₀ /Ag; Jung, I.H.; Jang, S.Y. High-efficiency low-temperature ZnO based perovskite solar cells based on highly polar, nonwetting self-assembled molecular layers. <i>Adv. Energy Mater.</i> 2018, 8, 1701683.	ITO/MPA-Ph- Ph-CA	1.10	-23.5	-81.0	-20.5	-	
49. Casalini, S.; Bortolotti, C.A.; Leonardi, F.; Biscarini, F. Self-assembled monolayers in organic electronics. <i>Chem. Soc. Rev.</i> 2017, 46, 40–71.	ITO/PQxD/FASnI ₃ /C ₆₀ /BCP/Ag	1.139	23.55	84.02	22.53	95%, 800 h, 45 °C ^{c,f}	
50. Lin, Y.; Firdaus, Y.; Isikgor, F.H.; Nugraha, M.I.; Yengel, E.; Harrison, G.T.; Hallani, R.; El-Labban, A.; Faber, H.; Mai, T.; et al. Self-Assembled Monolayer Enables Hole Transport Layer-Free Organic Solar Cells with 18% Efficiency and Improved Operational Stability. <i>ACS Energy Lett.</i> 2020, 5, 2935–2944.	ITO/TQxD/FASnI ₃ /C ₆₀ /BCP/Ag	0.574	21.05	68.8	8.3	90%, 1600 h ^{b,f}	[77]

^a maintained performance of its initial PCE after a specific time; ^b dark condition; ^c simulated 1 sun AM 1.5G illumination; ^d Tuning the work function of polar zinc oxide surfaces using modified phosphonic acid self-assembled monolayers. *Adv. Funct. Mater.* 2014, 24, 7014–7024.

2.5 Other SAMs

Besides the PA, CA, and CAA anchoring groups, several other anchoring groups have been introduced into SAMs (**Figure 4**). The photovoltaic properties of PSCs are summarized in **Table 4**.

52. Boissezon, R.; Muller, J.; Beaugeard, V.; Monge, S.; Robin, J.-J. Organophosphonates as anchoring agents onto metal oxide-based materials: Synthesis and applications. *RSC Adv.* 2014, 4, 35690–35707.
53. Ambrosio, F.; Martsinovich, N.; Troisi, A. What is the best anchoring group for a dye in a dye-sensitized solar cell? *J. Phys. Chem. Lett.* 2012, 3, 1531–1535.
54. Magomedov, A.; Al-Ashouri, A.; Kasparavicius, E.; Strazdaite, S.; Niaura, G.; Jošt, M.; Malinauskas, T.; Albrecht, S.; Getautis, V. Self-Assembled Hole Transporting Monolayer for Highly Efficient Perovskite Solar Cells. *Adv. Energy Mater.* 2018, 8, 1801892.
55. Al-Ashouri, A.; Magomedov, A.; Roš, M.; Jošt, M.; Taláíkis, M.; Chistiaková, G.; Bertram, T.; Márquez, J.A.; Köhnen, E.; Kasparavicius, E.; et al. Conformal monolayer contacts with lossless interfaces for perovskite single junction and monolithic tandem solar cells. *Energy Environ. Sci.* 2019, 12, 3356–3369.
56. Al-Ashouri, A.; Köhnen, E.; Li, B.; Magomedov, A.; Hempel, H.; Caprioglio, P.; Márquez, J.A.; Morales Vilches, A.B.; Kasparavicius, E.; Smith, J.A. Monolithic perovskite/silicon tandem solar cell with >29% efficiency by enhanced hole extraction. *Science* 2020, 370, 1300–1309.
57. Ullah, A.; Park, K.H.; Nguyen, H.D.; Siddique, Y.; Shah, S.F.A.; Tran, H.; Park, S.; Lee, S.I.; Lee, K.K.; Han, C.H.; et al. Novel Phenothiazine-Based Self-Assembled Monolayer as a Hole Selective Contact for Highly Efficient and Stable p-i-n Perovskite Solar Cells. *Figure 2. Molecules* 2021, 26, 2108475.
58. Wang, W.; Liu, X.; Wang, J.; Chen, C.; Yu, J.; Zhao, D.; Tang, W. Versatile Self-Assembled Molecule Enables High-Efficiency Wide-Bandgap Perovskite Solar Cells and Organic Solar Cells. *Adv. Energy Mater.* 2023, 13, 2300694.
59. Jiang, W.; Li, F.; Li, M.; Qi, F.; Lin, F.R.; Jen, A.K.Y. π -Expanded Carbazoles as Hole-Selective Self-Assembled HTM Device Structure Monolayers for Performance Perovskite Solar Cells. *Angew. Chem. Int. Ed.* 2022, 61, e202213560.
60. Li, E.; Liu, C.; Lin, H.; Xu, X.; Liu, S.; Zhang, S.; Yu, M.; Cao, X.M.; Wu, Y.; Zhu, W.H. Bonding Strength Regulates TPT Anchoring-Based Self-Assembly Monolayers for Efficient and Stable Perovskite Solar Cells. *Adv. Funct. Mater.* 2020, 31, 2103847.
61. Zhang, S.; Ye, F.; Wang, X.; Chen, R.; Zhang, H.; Zhan, L.; Jiang, X.; Li, Y.; Ji, X.; Liu, S. Minimizing buried interfacial defects for efficient inverted perovskite solar cells. *Science* 2023, 380, 404–409.

Table 4. Photovoltaic properties of PSCs using other SAMs.

62. Truong, M.A.; Funasaki, T.; Ueberricke, L.; Nojo, W.; Murdey, R.; Yamada, T.; Hu, S.; Akatsuka, A.; Sekiguchi, N.; Hira, Y. Self-Assembled Hole-Selective Derivative as a Face-On Oriented Hole-Collecting Monolayer for Efficient and Stable Inverted Perovskite Solar Cells. *J. Am. Chem. Soc.* 2023, 145, 7528–7539.

63. Ha, Y.E.; Jo, M.Y.; Park, J.; Kang, Y.-C.; Yoo, S.I.; Kim, J.H. Inverted Type Polymer Solar Cells with Self-Assembled POx-Monolayer Treated ZnO. *J. Phys. Chem. C* 2013, 117, 2646–2652.

64. Shi, Y.; Tan, L.; Chen, L.; Chen, Y. Alternative alcohol-soluble conjugated small molecule electrolytes for high-efficiency inverted polymer solar cells. *Phys. Chem. Chem. Phys.* 2015, 17, 3637–3646.

65. Arkan, E.; Yalcin, E.; Unal, M.; Arkan, M.Z.Y.; Can, M.; Tozlu, C.; Demic, S. Effect of functional groups of self-assembled monolayer molecules on the performance of inverted perovskite solar cell. *Mater. Chem. Phys.* 2020, 254, 123435.

66. Zuo, L.; Chen, Q.; De Marco, N.; Hsieh, Y.-T.; Chen, H.; Sun, P.; Chang, S.-Y.; Zhao, H.; Dong, S.; Yang, Y. Tailoring the interfacial chemical interaction for high-efficiency perovskite solar cells. *Nano Lett.* 2017, 17, 269–275.

a) maintained performance after initial PCE after a specific time; b) dark condition; c) simulated 1 Sun AM 1.5G illumination; d) relative humidity 30%; e) relative humidity 40%; f) inert gas; g) ambient air.

67. Aktas, E.; Cai, M.; Rodriguez-Seco, C.; Aktas, E.; Pudi, R.; Cambasud, W.; Demic, S.; Palomares, E. Semiconductor self-assembled monolayers as selective contacts for efficient PiN perovskite solar cells. *Energy Environ. Sci.* 2019, 12, 3003–3017.

3. Conclusions and Outlook

68. Li, E.; Bi, E.; Wu, Y.; Zhang, W.; Li, L.; Chen, H.; Han, L.; Tian, H.; Zhu, W.H. Synergistic Coassembly of Highly SAM-based HTMs have significantly increased PCEs in inverted PSCs. These SAMs, forming an ultrathin and uniform Wettable and Uniform Hole-Extraction Monolayers for Scaling-up Perovskite Solar Cells. *Adv. Funct. Mater.* 2019, 30, 1909509.

large-area processing, and the reduction in surface resistance and process costs. **Figure 5** shows the statistical distribution of PCE values of SAM-based PSCs depending on their PA, CA, and CAA anchoring groups.

69. Aktas, E.; Phung, N.; Köbler, H.; González, D.A.; Méndez, M.; Kafedjiska, I.; Turren-Cruz, S.-H.; Wenisch, R.; Lauermann, I.; Abate, A.; et al. Understanding the perovskite/self-assembled selective contact interface for ultra-stable and highly efficient p-i-n perovskite solar cells. *Energy Environ. Sci.* 2021, 14, 3976–3985.

70. Aktas, E.; Pudi, R.; Phung, N.; Wenisch, R.; Gregori, L.; Meggiolaro, D.; Flatken, M.A.; De Angelis, F.; Lauermann, I.; Abate, A.; et al. Role of Terminal Group Position in Triphenylamine-Based Self-Assembled Hole-Selective Molecules in Perovskite Solar Cells. *ACS Appl. Mater. Interfaces* 2022, 14, 17461–17469.

71. Hung, C.M.; Mai, C.L.; Wu, C.C.; Chen, B.H.; Lu, C.H.; Chu, C.C.; Wang, M.C.; Yang, S.D.; Chen, H.C.; Yeh, C.Y. Self-Assembled Monolayers of BI Functionalized Porphyrins: A Novel Class of Hole-Layer-Coordinating Perovskites and Indium Tin Oxide in Inverted Solar Cells. *Angew. Chem. Int. Ed.* 2023, 135, e202309831.

72. Li, W.; Cariello, M.; Méndez, M.; Cooke, G.; Palomares, E. Self-Assembled Molecules for Hole-Selective Electrodes in Highly Stable and Efficient Inverted Perovskite Solar Cells with Ultralow Energy Loss. *ACS Appl. Energy Mater.* 2023, 6, 1239–1247.

73. Wu, T.; Wang, Y.; Dai, Z.; Wu, Y.; Wang, T.; Meng, X.; Bi, E.; Yang, X.; Han, L. Efficient and stable CsPbI₃ solar cells via regulating lattice distortion with surface organic terminal groups. *Adv. Mater.* 2019, 31, 1900605.

74. Wang, Y.; Liao, Q.; Chen, J.; Huang, W.; Zhuang, X.; Tang, Y.; Li, B.; Yao, X.; Feng, X.; Zhang, X. Teaching an old anchoring group new tricks: Enabling low-cost, eco-friendly hole-transporting materials for efficient and stable perovskite solar cells. *J. Am. Chem. Soc.* 2020, 142, 16632–16643.

75. Liao, Q.; Wang, Y.; Hao, M.; Li, B.; Yang, K.; Ji, X.; Wang, Z.; Wang, K.; Chi, W.; Guo, X.; et al. Green-Solvent-Processable Low-Cost Fluorinated Hole Contacts with Optimized Buried Interface for Highly Efficient Perovskite Solar Cells. *ACS Appl. Mater. Interfaces* 2022, 14, 43547–43557.

76. Zhang, S.; Wu, R.; Wang, C.; Han, Y.; Wu, Y.; Zhang, W. H. Comjugated Self-Assembled Monolayer as Stable Hole-Selective Contact for Inverted Perovskite Solar Cells. *ACS Mater. Lett.* 2022, 4, 1976–1983.

77. Afraj, S.N.; Kuan, C.H.; Lin, J.S.; Ni, J.S.; Velusamy, A.; Chen, M.C.; Diau, E.W.G. Quinoxaline-Based X-Shaped Sensitizers as Self-Assembled Monolayer for Tin Perovskite Solar cells. *Adv. Funct. Mater.* 2023, 33, 2213939.

78. Guo, H.; Liu, C.; Hu, H.; Zhang, S.; Ji, X.; Cao, X.-M.; Ning, Z.; Zhu, W.-H.; Tian, H.; Wu, Y. Neglected acidity pitfall: Boric acid-anchoring hole-selective contact for perovskite solar cells. *Natl. Sci. Rev.* 2023, 10, nwad057.